

Neuroinflammation and its relationship to changes in brain volume and white matter lesions in multiple sclerosis

| | |
|---|--|
| Journal: | <i>Brain</i> |
| Manuscript ID | BRAIN-2017-00437.R2 |
| Manuscript Type: | Original Article |
| Date Submitted by the Author: | 28-Jun-2017 |
| Complete List of Authors: | Datta, Gourab; Imperial College London, Brain Sciences Colasanti, Alessandro; Imperial College London, Division of Brain Sciences; Imanova Centre for Imaging Sciences, Gunn, Roger; Imanova Centre for Imaging Sciences, Malik, Omar; Imperial College Healthcare NHS Trust, Ciccarelli, Olga; UCL Institute of Neurology, Brain Repair and Rehabilitation Nicholas, Richard; Imperial College Faculty of Medicine, Department of Cellular & Molecular Neuroscience Van Vlierberghe, Eline; ICOMETRIX Van Hecke, Wim; Antwerp University Hospital, Department of Radiology; Icometrix, Searle, Graham; Imanova Ltd., Santos-Ribeiro, Andre; Imperial College London, Brain Sciences Matthews, Paul M; Imperial College London, |
| Subject category: | Multiple sclerosis and neuroinflammation |
| To search keyword list, use whole or part words followed by an *: | Microglia < NEURODEGENERATION: CELLULAR AND MOLECULAR, MULTIPLE SCLEROSIS AND NEUROINFLAMMATION, MS: imaging < MULTIPLE SCLEROSIS AND NEUROINFLAMMATION, White matter lesion < MULTIPLE SCLEROSIS AND NEUROINFLAMMATION, Neuroinflammation < MULTIPLE SCLEROSIS AND NEUROINFLAMMATION |
| | |

SCHOLARONE™
Manuscripts

Neuroinflammation and its relationship to changes in brain volume and white matter lesions in multiple sclerosis

G. Datta¹, A. Colasanti^{1,2}, E.A. Rabiner^{3,4}, R. N. Gunn^{1,3}, O. Malik¹, O. Ciccarelli^{5,6}, R. Nicholas¹, E. Van Vlierberghe⁷, W. Van Hecke⁷, G. Searle^{1,3}, A. Santos-Ribeiro¹, P.M. Matthews¹

¹Division of Brain Sciences, Imperial College London, UK

²Department of Neuroscience, Brighton and Sussex Medical School, UK

³Imanova Ltd, London, UK

⁴Centre for Neuroimaging Sciences, King's College, London, UK

⁵Queen Square Multiple Sclerosis Centre, University College London, Institute of Neurology, London, UK

⁶NIHR University College London Hospitals Biomedical Research Centre, London, UK

⁷Icometrix, Boston, USA

Running Title: A longitudinal study of TSPO PET and MRI in MS

Word count:

Running title (characters) 37 characters

Abstract 311

Main text 5210

Tables: 2

Figures: 5

Address for correspondence:

Prof. Paul M. Matthews

p.matthews@imperial.ac.uk

E515, Division of Brain Sciences

Department of Medicine

Hammersmith Hospital

Du Cane Road, London WC12 0NN

Tel: 0044 207 594 2855

Abstract

Brain MRI is an important tool in the diagnosis and monitoring in multiple sclerosis patients. However, MRI alone provides limited information for predicting an individual patient's disability progression. In part, this is because MRI lacks sensitivity and specificity for detecting chronic diffuse and multi-focal inflammation mediated by activated microglia/macrophages. The aim of this study was to test for an association between 18 kDa translocator protein (TSPO)-brain positron emission tomography (PET) signal, which arises largely from microglial activation, and measures of subsequent disease progression in multiple sclerosis patients. 21 multiple sclerosis patients (7 with secondary progressive disease and 14 with a relapsing remitting disease course) underwent T1- and T2-weighted and magnetization transfer MRI at baseline and after 1 year. PET scanning with the translocator protein radioligand [^{11}C]PBR28 was performed at baseline. Brain tissue and lesion volumes were segmented from the T1- and T2-weighted MRI and relative [^{11}C]PBR28 uptake in the normal-appearing white matter was estimated as a distribution volume ratio (DVR) with respect to a caudate pseudo-reference region. Normal appearing white matter distribution volume ratio DVR at baseline was correlated with enlarging T2-hyperintense lesion volumes over the subsequent year ($\rho=0.59$, $p=0.01$). A *post hoc* analysis showed that this association reflected behaviour in the sub-group of relapsing remitting patients ($\rho=0.74$, $p=0.008$). By contrast, in the sub-group of secondary progressive patients, microglial activation at baseline was correlated with later progression of brain atrophy ($\rho=0.86$, $p=0.04$). A regression model including the baseline normal-appearing white matter distribution volume ratio DVR, T2 lesion volume and normal-appearing white matter magnetization transfer ratio for all of the patients combined explained over 90% of the variance in enlarging lesion volume over the subsequent 1 year. Glial activation in white matter assessed by translocator protein PET significantly improves predictions of white matter lesion enlargement in relapsing remitting patients and greater brain atrophy in secondary progressive disease over a period of short-term follow up.

Keywords: multiple sclerosis; microglia; atrophy; translocator protein; positron emission tomography

Abbreviations: DVR = distribution volume ratio; MTR = magnetization transfer ratio; NAWM = normal appearing white matter; PET = positron emission tomography; RRMS = relapsing remitting multiple sclerosis; SPMS = secondary progressive multiple sclerosis; TSPO = translocator protein

Introduction

Multiple sclerosis is a chronic inflammatory, demyelinating and neurodegenerative disease of the central nervous system leading to progressive neuroaxonal loss and subsequent brain atrophy. Clinically, multiple sclerosis typically presents as acute neurological episodes (relapses) with complete or partial recovery (relapsing remitting multiple sclerosis or RRMS) with a later stage of progression of disability (secondary progressive multiple sclerosis or SPMS). Inflammatory demyelinating white (and grey) matter lesions are characteristic of the disease. White matter lesions are visualized on conventional MRI by focal hyperintensity on T2-weighted imaging and, when acute, often by gadolinium-contrast enhancement on T1-weighted imaging. White matter lesions detected by MRI are routinely used to aid diagnosis and monitor disease. Combination of the number of new and enlarging T2 lesions with annualized brain atrophy rate predicts a large proportion of the variance in short term disability progression for RRMS (Sormani *et al.*, 2011; Popescu *et al.*, 2013; Sormani *et al.*, 2014). These conventional MRI measures are commonly used as early phase clinical trial outcomes (Filippi *et al.*, 1995; Lee *et al.*, 1998). We hypothesize that imaging measures of activation of microglia, the innate immune cells of the central nervous system, could predict an additional component of the variance in future disease progression with both RRMS and SPMS.

Histopathologically different types of white matter lesions have been identified (Lucchinetti *et al.*, 2004). Acute lesions or those showing peripheral innate immune activation associated with demyelination (so called “slowly expanding” lesions) may be those most likely to enlarge over time (Prineas *et al.*, 2001; Lucchinetti *et al.*, 2004; Filippi *et al.*, 2012). The latter appear to be characteristic of progressive forms of MS. Activated microglial nodules in the white matter that can be found in association with demyelinating and damaged axons may precede the appearance of new lesions (Seewann *et al.*, 2009; Singh *et al.*, 2013). Direct tests and clinical applications of these findings is limited, however, as conventional MRI lacks sensitivity and specificity for detecting the diffuse extra-lesional innate immune inflammation in the white matter evident from *post-mortem* neuropathology (Filippi *et al.*, 2012); radiologically, these areas appear as normal appearing white matter (NAWM) on conventional MRI (Allen *et al.*, 2001). A challenge for imaging in MS thus has been to develop more sensitive and specific measures to better reconcile assessments of histopathology made *post mortem* with imaging measures *in vivo*. Magnetization transfer imaging, for example, enhances the contrast between white matter water molecules associated with macromolecules and free water. This increases sensitivity for detection of demyelination and neuroaxonal loss (Schmierer *et al.*, 2004; Vrenken *et al.*, 2006; Moll *et al.*, 2011).

Our understanding of the *in vivo* evolution of innate inflammatory pathology in multiple sclerosis brain remains limited, however. This aspect of the immune response has mainly been studied only cross-sectionally *post mortem*. The 18 kDa mitochondrial translocator protein can be highly expressed in activated microglia and astrocytes (Cosenza-Nashat *et al.*, 2009). In multiple sclerosis, currently available imaging-pathological correlations suggest that increased radioligand uptake relatively specifically reflects microglial activation (Matthews and Datta, 2015; Datta *et al.*, 2016). PET radioligands specific for TSPO have been

4

used to study the distribution and relative magnitude of microglial activation. Clinical TSPO PET studies reported higher uptake in grey matter and white matter (NAWM and white matter lesions) in multiple sclerosis than in healthy volunteers, although the relationship of TSPO uptake across brain regions within individual multiple sclerosis brains was not reported in these studies (Politis *et al.*, 2012; Colasanti *et al.*, 2014; Herranz *et al.*, 2016). These findings *in vivo* were obtained using both the first generation and the higher affinity second generation TSPO radioligands.

Increases in lesion load and brain atrophy are strongly correlated with disease progression and worse clinical outcomes (Sormani *et al.*, 2014). Here we investigated whether *in vivo* glial activation assessed using [¹¹C]PBR28 TSPO PET imaging could be used to predict T2 lesion volume change and brain atrophy over the subsequent 1 year and therefore enhance precision in identifying patients at higher risk of worsening disease. We explored whether adding magnetization transfer imaging of NAWM as a measure of demyelination could further add additional predictive power.

Materials and methods

Patients

The study was approved by the West Bromley Research Ethics Committee (Ref No. 14/LO/0445) and the UK Administration of Radioactive Substances Advisory Committee. All patients gave written informed consent in accordance with the Declaration of Helsinki.

Patients with a diagnosis of multiple sclerosis according to the revised McDonald criteria (2010) (Polman *et al.*, 2011), with EDSS (Expanded Disability Status Scale) up to 7.0 and either a relapsing remitting or a secondary progressive disease course were studied (Table 1). Usual care of the patients was not interrupted during the period of this observational study and many of the patients were on disease modifying treatments (Table 1), but none of the patients had been treated with steroids or experienced a clinical relapse within 3 months of their scans. Patients who were claustrophobic, had metal implants or fragments in their bodies or who had received radiation above background exceeding 10 millisieverts in the previous 3 years or women who were pregnant or breastfeeding were not eligible to participate, although none of those screened met these exclusion criteria and were therefore not excluded.

MRI scanning was performed at baseline and after 1 year and a PET scan was done at baseline only. The same scanner, MRI parameters, and clinical assessment protocols were employed for all participants and longitudinal comparisons.

EDSS and neurological assessment

The clinical history and physical examination, including assessment of EDSS, was completed by the same investigator (GD) on every patient subject at the screening visit and after 1 year at the time of follow-up MRI scanning for each of the subsequent study visits. The first study visit, at which all the baseline scans

Formatted: Font color: Red

Formatted: Font color: Red

were performed, took place within 6 weeks of the screening visit. None of the patients experienced clinical events between their screening and baseline scanning visits. ~~A follow-up MRI scan was performed after 12 months.~~

TSPO genotyping

TSPO genotype was assessed using a TaqMan based polymerase chain reaction (Applied Biosystems® QuantStudio™ 7) assay specific for the rs6971 polymorphism in the TSPO gene, as previously described (Owen *et al.*, 2012). Participants having genotypes associated with low affinity binding were excluded, as they show negligible displaceable binding (Owen *et al.*, 2012). For the baseline scans, there were 13 high affinity binders and 11 medium affinity binders.

MRI scanning

MRI scans were performed on a Siemens 3 Tesla Trio scanner (Siemens Healthcare, Erlangen Germany) equipped with a 32-channel phased-array head coil. Volumetric T1-weighted MPRAGE images were acquired for all patients using a 1 mm isotropic resolution 3D SPACE sequence (repetition time = 2300 ms, echo time = 2.98 ms, inversion time = 900 ms with 256 x 240 x 160mm field of view), before and 5 minutes after intravenous gadolinium-chelate administration (0.2 mL/kg Gadoteric Acid, Dotarem®) (Jack *et al.*, 2008). Volumetric T2-weighted FLAIR (fluid attenuated inversion recovery) images were acquired using a 1mm isotropic resolution 3D SPACE sequence with a 250 x 250 x 160 mm field of view, echo time = 395 ms, repetition time = 5 s, inversion time = 1800 ms, turbo factor of 141, 256 x 256 x 160 matrix, and parallel imaging factor of 2).

MTR maps were acquired using a 3D spoiled gradient echo sequence (fast low angle shot [FLASH]). To generate a pseudo- proton density weighting (PDw) image, two volumes with 1mm isotropic resolution were acquired using 256x246x196 mm field of view, repetition time TR=27 ms, flip angle=5°, a parallel imaging factor of 2, 6 echoes acquired using 630Hz/pixel bandwidth with TEs every 1.95ms from 1.95 to 11.7ms). Magnetization transfer weighting (MTw) was added using a 12.24ms duration Gaussian radiofrequency RF pulse (flip angle of 540) 2.2 kHz off resonance. MTR maps were calculated from the equation:

$$MTR = 100 * (S_{PDw} - S_{MTw}) / S_{PDw}$$

where S_{PDw} =signal from PDw image and S_{MTw} =signal from MTw image

PET scanning

PET scanning (Discovery RX PET/CT scanner) was performed with a trans-axial resolution of 5.0 mm, and a radial resolution of 5.1 mm. PET data were reconstructed using filtered back projection including corrections for attenuation and scatter (based on a low-dose CT acquisition). The dynamic data were binned into 26 frames (durations of 8 x 15 s, 3 x 1 min, 5 x 2 min, 5 x 5 min, 5 x 10 min). [¹¹C]PBR28 was injected as an intravenous bolus over approximately 20 s at the start of a 90 min dynamic PET acquisition. Injected

Formatted: Font color: Red

6

activities for [^{11}C]PBR28 ranged from 223.8- 379.6 MBq (335.1 ± 30.9 MBq, $n=24$). Injected mass for different **patient subjects** ranged from 1.48 - 8.91 μg (3.35 ± 1.96 μg).

Radioligand synthesis

Radiosynthesis and quality control was performed on site according to the method of Briard et al. (2008) with modification, as previously described, obtaining radiochemical purities of $> 95\%$ (Briard *et al.*, 2008).

MRI image and PET kinetic analyses

T2 FLAIR images were rigidly registered to T1 using FLIRT (FMRIB Software Library v5.0). White matter lesions were manually segmented on the registered T2 image using Jim software (Xinapse Systems v7). The white matter lesion mask was used for lesion- filling the baseline and follow-up T1 images before segmentation into white matter, grey matter, cerebral cortex and cerebrospinal fluid using the FSL tools FAST and FIRST (FMRIB Software Library v5.0) (Battaglini *et al.*, 2012). Normalised brain volumes were calculated using SIENAX (Smith *et al.*, 2002). For measurement of longitudinal changes in brain volumes, the MSmetrix method was used (Jain *et al.*, 2015; Smeets *et al.*, 2016). In brief, the baseline and follow-up T1 images were bias corrected, lesion filled, and skull stripped, followed by linear and a non-linear registration from baseline to follow-up and visa versa. Voxel-wise differences in volume from the nonlinear registration were integrated over the whole brain and grey matter volumes to calculate the changes in volume over 1 year, as previously described (Smeets *et al.*, 2016).

T2 hyperintense white matter lesions were segmented automatically using a previously validated method (Jain *et al.*, 2015). Subtraction of the lesion masks from the MRI scans acquired at baseline from that acquired after 1 year for each **patient subject** allowed new or enlarging lesion volumes to be determined. For this, a mask of NAWM was created by subtracting a white matter lesion mask dilated by 6mm around its edges in 3D from the FAST segmentation of the total white matter and then eroding the resulting mask further by 3 mm (Lee *et al.*, 1998).

The T1 image, NAWM mask and white matter lesion mask and dynamic PET images were used as inputs to the MIAKAT software package (www.miakat.org) for kinetic analysis of PET data. Using this software, PET images were corrected for **patient subject** motion using a frame-by-frame realignment algorithm and rigid registered to MNI (Montreal Neurological Institute) 2 mm space using SPM5 (Wellcome Trust Centre for Neuroimaging, <http://www.fil.ion.ucl.ac.uk/spm>) with a mutual information cost function. The Clinical Imaging Centre Neuroanatomical Atlas (Tziortzi *et al.*, 2011) was non-linearly deformed into the individual's space, via mapping of T1-weighted MR imaging data, to obtain a personalized anatomical parcellation of the brain. This parcellation was used to generate time-activity curves for regions of interest, including the thalamus, caudate, NAWM, white matter lesions and (voxel-wise) for whole brain.

The Logan graphical reference method was used to estimate DVR values from regional and voxel-wise time-activity curves using the caudate nucleus as a pseudo-reference region and a linear start time of 35

7

minutes (Logan *et al.*, 1996). With this approach, a distribution volume ratio (DVR) can be estimated from a graphical linearization method using dynamic PET measurements from the region of interest $C(t)$ and from a reference region $C'(t)$ with an average rate constant for radioligand clearance from tissue-to-plasma of k'_2 :

$$\frac{\int_0^T C(t) dt}{C(T)} = DVR \left[\frac{\int_0^T C'(t) dt + C'(T)/k'_2}{C(T)} \right] + \text{int}'$$

In this graph, DVR is the regression slope and the intercept is int' .

Statistical analyses

Statistical analyses were performed using SPSS software (IBM, SPSS v22). For correlational analyses, the Spearman's correlation coefficient was calculated, unless otherwise stated. Descriptive statistics were reported as median and range, unless otherwise stated.

The proportional increase in volume from baseline T2 lesion volume was less than 10% for almost all patients with enlarging T2 lesions, so we considered a 5% increase in volume of enlarging T2 lesions as a significant outcome change in constructing a receiver operating characteristic (ROC) with white matter DVR as the discriminant.

Hierarchical linear regression was used to assess separately whole brain atrophy rate, overall T2 lesion volume change and enlarging T2 lesion volume. We evaluated 4 different 3 level hierarchical linear regression models:

1. Dependent variable of whole brain atrophy rate (% between baseline and follow-up scan) with EDSS, age and gender as covariates (level 1) and independent variables as NAWM DVR controlling for TSPO binding status (level 2) followed by baseline T2 lesion volume (level 3).
2. Dependent variable of overall T2 lesion volume change (mL between baseline and follow-up scan) with three levels as above.
3. Dependent variable of enlarging T2 lesion volume change (mL between baseline and follow-up scan) with three levels as above.
4. Dependent variable of enlarging T2 lesion volume change (mL between baseline and follow-up scan) with NAWM DVR controlling for TSPO binding status (level 1), NAWM MTR (level 2) and baseline T2 lesion volume (level 3).

For all models, the coefficient of determination (R^2) was reported for level 1. For each level thereafter (level 2 and 3), the contribution of the next level independent of other levels for explaining variance in the dependent variable was reported as R^2 change values. Where correlations were directly assessed and for *post*

hoc analyses, a correction was made for multiple comparisons (Bonferroni method). A p-value of less than 0.05 was considered significant for all statistical tests. Receiver operator characteristic (ROC) plots were used to assess the accuracy of classifications using the models.

Results

24 multiple sclerosis patients initially underwent [¹¹C]PBR28 PET scanning and MRI at baseline (17 RRMS and 7 SPMS). Clinical characteristics of the participants are summarised in Table 1. [¹¹C]PBR28 PET imaging characteristics of their white matter and of individual lesions are described relative to white matter of matched, healthy volunteers in a recent paper (Datta *et al.*, 2017). Illustrative images are shown in Figure 1. One patient from this group was lost to follow-up (A23), one withdrew consent (A9) and one declined scanning because of discomfort from side effects of treatment with alemtuzimab (A22). 21 patients had a follow-up MRI approximately 1 year (median 12 months, range 11-14 months) after the baseline scanning. Of the 21 patients included in the longitudinal analysis (8 men; median age 48 years, range 22–66 years), 7 had a diagnosis of SPMS and 14 of RRMS. The median baseline EDSS was 4.0 (range, 1.0–7.0) and median disease duration was 13 years (range, 1-28 years). 7 patients had a relapse between their baseline and follow-up scans (median 0 relapses/year, range 0-1 relapses/year). The EDSS at follow-up did not change in 16 patients of the 21 patients (EDSS change: median 0.0, mean 0.2, range 0.0-2.0).

[¹¹C]PBR28 DVR measures predict subsequent radiological progression of disease

Baseline TSPO PET DVR measures from T2 hyperintense lesions, the NAWM and grey matter and changes in T2 lesions and whole brain or grey matter volume over 1 year were assessed for each patient (Table 2). The baseline NAWM DVR and the MRI volume measures at baseline and longitudinally are summarised in Table 2. NAWM and white matter lesion DVR were positively correlated with enlarging T2 lesion volume ($\rho=0.59$, $p=0.01$; $\rho=0.64$, $p=0.004$, respectively) over the subsequent 1 year. A *post hoc* analysis suggested that this relationship was specific for the sub-group of patients with RRMS, who showed strong relationships between both baseline NAWM and white matter lesion DVR and enlarging T2 lesion volumes ($\rho=0.74$, $p=0.008$; $\rho=0.64$, $p=1 \times 10^{-3}$, respectively) (Figure 2A). By contrast, we did not find the associations between either the enlarging T2 lesion volume and NAWM DVR ($\rho= -0.05$, $p=0.91$) or white matter lesion DVR ($\rho= -0.41$, $p=0.36$) in the sub-group of SPMS patients. However, correlations were observed in the SPMS patients between white matter lesion DVR and both subsequent changes in whole brain ($\rho=0.86$, $p=0.04$) and grey matter ($\rho=0.96$, $p=5 \times 10^{-4}$) volumes (Figure 2B). A trend towards correlation between NAWM DVR and whole brain volume change over the subsequent 1 year also was found in the SPMS patients ($\rho=0.71$, $p=0.07$) as part of this *post hoc* exploratory analysis, although it did not reach statistical significance. A similar analysis for the RRMS group did not identify associations between DVR and either whole brain or grey matter volume changes.

NAWM and white matter lesion DVR at baseline were not associated with total T2 lesion volume changes (the mean of contributions from both enlarging and shrinking lesions) between baseline and follow-up (Spearman's $\rho = -0.08$, $p = 0.75$ and $\rho = -0.01$, $p = 0.95$, respectively), nor were there significant associations between DVR and the total T2 lesion volume change in either the RRMS or SPMS sub-groups. We also did not find evidence for associations between NAWM and white matter lesion DVR at baseline and subsequent changes in whole brain ($\rho = -0.006$, $p = 0.98$; $\rho = 0.08$; $\rho = 0.74$, respectively) or total grey matter ($\rho = 0.07$; $\rho = 0.78$; $\rho = 0.15$; $\rho = 0.51$, respectively) volumes for the group of multiple sclerosis patients as a whole.

Stratifying patients for enlarging T2 lesion activity using baseline NAWM [¹¹C]PBR28 DVR

We explored whether differences in NAWM DVR at baseline could be used to stratify patients at higher risk of enlarging T2 lesion volumes over the subsequent year. We estimated the optimal NAWM DVR discriminating higher and lower risk of enlarging T2 lesion volume by constructing an ROC curve with NAWM DVR as the test variable. The discriminant value of baseline NAWM DVR that best discriminated between patients with an enlarging, rather than a decreasing or stable, T2 lesion volume was determined: NAWM DVR cut-off of 1.10 maximised specificity (67%) and sensitivity (67%) for discriminating a >5% increase. With this discriminant, there was an approximately 30% greater relative increase in enlarging T2 hyperintense volumes in the higher (median 4.8 mL, range 1.1-10.6 mL) than in the lower (median 6.8 mL, range 0.7-9.6 mL) NAWM DVR sub-group ($p = 0.04$, Mann-Whitney test) (Figure 3).

Multivariate models predicting subsequent changes in MRI measures of disease progression

We explored models predicting future disease activity based on demographic, clinical and MRI data, as well as PET measures at baseline. We initially modelled the whole brain volume change between the baseline and follow-up MRI scans as a function of EDSS, age and gender ($R^2 = 0.48$, $p = 0.01$). Neither the baseline NAWM DVR (controlling for TSPO binding status) nor the baseline T2 lesion volume improved the main model (R^2 change = 0.09, $p = 0.26$ and R^2 change < 0.01, $p = 0.97$, respectively). Overall T2 lesion volume change was not predicted by either the main model with variables EDSS, age, gender ($p = 0.68$) or any of the subsequent levels of the hierarchical model described in the Methods (R^2 change = 0.02, $p = 0.87$).

We then explored models of the enlarging T2 lesion volume. EDSS, age and gender alone did not predict future enlarging T2 lesion volume well ($R^2 = 0.33$, $p = 0.14$). Including the baseline NAWM DVR added significant explanatory power to the model (R^2 change = 0.37, $p = 0.004$). A hierarchical regression model with the first level as NAWM DVR accounted for approximately 50% of the variance in enlarging T2 lesion volumes ($R^2 = 0.46$, $p = 0.001$). We additionally explored inclusion of the baseline T2 lesion volume (R^2 change = 0.30, $p = 5 \times 10^{-6}$) and NAWM MTR (R^2 change = 0.12, $p = 0.04$) and found that it improved the model prediction.

Correlations between baseline [¹¹C]PBR28 DVR and MRI measures of disease burden

10

To place these longitudinal observations in context, we tested for correlations between the [^{11}C]PBR28 DVR and MRI measures of disease burden at baseline, extending our previous observations (Datta *et al.*, 2017). Both NAWM and white matter lesion DVR were positively correlated with the baseline T2 lesion volume ($\rho=0.49$, $p=0.03$ and $\rho=0.63$, $p=0.002$, respectively). The baseline NAWM MTR was negatively correlated with NAWM DVR ($\rho=-0.69$, $p=8\times 10^{-4}$). NAWM and white matter lesion DVR were negatively correlated with baseline whole brain volume ($\rho=-0.81$, $p=4\times 10^{-5}$ and $\rho=-0.74$, $p=4\times 10^{-4}$, respectively). NAWM DVR was correlated with baseline normalised grey matter volume ($\rho=-0.56$, $p=0.02$) (Figure 4), but we did not find a statistically significant association between white matter lesion DVR and grey matter volume at baseline ($\rho=-0.49$, $p=0.08$).

We also tested for relationships between [^{11}C]PBR28 DVR inflammatory measures across tissue compartments in the PET scan conducted at baseline. NAWM DVR was correlated strongly with the mean DVR of T2 white matter lesions (Spearman's $\rho=0.92$, $p=3\times 10^{-10}$) and the mean cortical ($\rho=0.93$, $p=1\times 10^{-10}$) and thalamic ($\rho=0.79$, $p=1\times 10^{-5}$) DVR (Figure 5).

Discussion

We investigated *in vivo* glial activation in the white matter of multiple sclerosis patients using the second generation TSPO ligand, [^{11}C]PBR28, and its relationship to subsequent changes in MRI over 1 year. We found that the [^{11}C]PBR28 DVR in NAWM was highly correlated with DVR in T2 white matter lesions, whole cortex and the thalamus. NAWM and white matter lesion DVR were correlated with T2 lesion volume and whole brain volume at baseline. Enlarging T2 lesions and brain atrophy rates have prognostic significance for development of disability progression in multiple sclerosis (Sormani *et al.*, 2014). We found that the white matter [^{11}C]PBR28 DVR at baseline was correlated with the subsequent enlarging T2 lesion volume. A model including baseline NAWM DVR and NAWM MTR significantly improved prediction of future disease activity (enlarging T2 lesion volume) over the subsequent year relative to that estimated using only clinical and conventional MRI measures.

We found that patients with a higher level of glial activation in the NAWM had increased microglial activation in white matter lesions and grey matter volumes. While *post mortem* studies have found only a weak correlation between white matter and grey matter lesion volumes, these studies have not addressed the innate immune activation accompanying them (Calabrese *et al.*, 2015). They also have not included consideration of the potentially extensive, dynamically evolving meningeal inflammation (Lucchinetti *et al.*, 2011; Popescu and Lucchinetti, 2012; Absinta *et al.*, 2015). Previous *in vivo* TSPO PET studies have found evidence for diffuse glial activation in grey and white matter of multiple sclerosis patients, relative to healthy controls (Filippi *et al.*, 2012; Politis *et al.*, 2012; Colasanti *et al.*, 2014; Rissanen *et al.*, 2014; Giannetti *et al.*, 2015; Datta *et al.*, 2016; Datta *et al.*, 2017). Common genetic and environmental factors may contribute to the expression of brain inflammation throughout the brain and, through this, to disease progression (Zivadinov *et al.*, 2009; Mowry *et al.*, 2012; Gourraud *et al.*, 2013). The strong correlations in

innate immune activation across brain tissue compartments defined by TSPO radioligand binding suggest that it may be most useful to consider central nervous system-wide immune activation for understanding individual differences in disease severity or progression, rather than that in any single tissue compartment (either white or grey matter).

We found correlations between baseline whole brain volume and T2 lesion load with both the [¹¹C]PBR28 DVR in NAWM and in white matter T2 lesions. A previous TSPO PET study reported correlations of NAWM TSPO ligand binding with baseline brain volume measures in SPMS (Versijpt *et al.*, 2005). This and related associations identified in cross-sectional studies have been interpreted to suggest that the diffuse microglial activation either contributes causally- or reflects a response- to neuroaxonal loss. With a longitudinal design, we were able to investigate the associations between microglial activation and measures of inflammatory activity and neuroaxonal loss more directly. We found that a measure of higher levels of microglial activation was associated with a greater volume of subsequently enlarging lesions in the RRMS sub-group. By contrast, in the sub-group of patients with SPMS, microglial activation was associated not with enlarging T2 hyperintense lesions in the white matter, but with greater subsequent brain atrophy. A limitation of our study is that it was not powered to assess the multivariate hierarchical regression models separately for sub-groups of RRMS and SPMS patients. These associations also suggest that innate immune activation contributes to future inflammatory neurodegeneration, but do not rule out the possibility that the association is a *response* to neurodegeneration, rather than a *cause*. To test this confidently, longitudinal assessment of responses to an intervention that selectively modulates the diffuse microglial activation is needed.

Nonetheless, there is evidence that some or all of the microglial activation measured here is contributing to neurodegeneration. Activated nodules of microglia have been detected in extra-lesional white matter both in association with demyelinating axons and in the absence of myelin loss (van Horssen *et al.*, 2012; Singh *et al.*, 2013). Pre-clinical studies support a role for microglial activation being pro-inflammatory in multiple sclerosis and contributing to neurodegeneration (see e.g., (Duffy *et al.*, 2014)). ~~More indirectly,~~ Previous work suggested that white matter MTR **as a sensitive *in vivo* marker of neurodegeneration (combined neuro-axonal loss and demyelination)** predicts future disease progression (Agosta *et al.*, 2006). We found that [¹¹C]PBR28 NAWM DVR was negatively correlated with NAWM MTR. We had observed this also in a previous study using another second generation TSPO ligand ([¹⁸F]PBR111), which showed higher TSPO binding in the NAWM with lower MTR (Colasanti *et al.*, 2014).

Short-term disability progression is predicted well by a combination of the whole brain atrophy rate and the numbers of new and enlarging T2 lesions over 6-12 months (Popescu *et al.*, 2013; Sormani *et al.*, 2014). Here we constructed a model for prediction of future disease activity based on NAWM DVR, NAWM MTR and T2 lesion volumes measured at a *single* time point. This model explained over 90% of the variance in enlarging lesion volumes over the subsequent 1 year. This is consistent with the hypothesized association between diffuse innate immune activation in white matter and new T2 lesions and histopathological

interpretations of white matter lesions having prominent microglial activation at their edges as enlarging lesions (Lucchinetti *et al.*, 2004; Filippi *et al.*, 2012).

There are limitations to our study. First, feasibility limited the number of patients. Our study also included a mixed population of multiple sclerosis patients (many of who were receiving disease modifying treatments) with a follow-up of approximately 1 year. **The group of RRMS patients was very heterogenous (EDSS from 1 to 7 and DD from 1 to 28 years)**. With the smaller population size and short duration of follow-up, we did not detect any new T2 lesions and there were few relapses and little overall EDSS change across the group. This is not uncommon with relatively short follow-up periods for patients on treatment (Goldman *et al.*, 2010). We did not attempt to directly assess relationships between microglial activation and the appearance of new lesions in the grey matter, as 3Tesla MRI appears relatively insensitive to cortical lesions (Geurts *et al.*, 2005; Klaver *et al.*, 2013). This question may be better addressed in the future using ultra-high MRI (Klaver *et al.*, 2013). We also did not compare the longitudinal changes in brain volumes between MS patients and well-matched healthy volunteers, although it is well established that regional and global brain atrophy rates are greater in MS patients than healthy people (Barkhof *et al.*, 2009). A future study including healthy volunteers or an appropriate healthy, historical comparator group also would enhance the clinical meaningful of observations by testing directly whether increased microglial activation is associated with rates of brain atrophy in patients that are significantly greater than in a matched healthy control group. Finally, our conclusions regarding differential responses in the sub-groups with RRMS and SPMS were based on *post hoc* analyses. TSPO PET studies including larger numbers of progressive multiple sclerosis patients and patients of longer duration are needed. Further analysis focusing on individual lesional [¹¹C]PBR28 DVR and MTR could provide insights into how microglial activation relates to future changes in the balance of remyelination and demyelination within individual lesion volumes.

Available neuropathology and a recent combined magnetic resonance spectroscopic and TSPO PET study suggest that microglial activation likely makes the dominant contribution to the higher TSPO PET signal in people with multiple sclerosis (Matthews and Datta, 2015; Datta *et al.*, 2016). Our results demonstrate strong correlations between the diffuse glial activation measured by TSPO PET in white and grey matter, despite the lack of a strong association between focal lesional activity in white and grey matter (Bo *et al.*, 2007). While we cannot be confident of the mechanisms mediating the relationships observed, our results provide evidence that the microglial activation assessed by TSPO is meaningful clinically. Our study suggests that greater activation in the NAWM is a marker of greater risk of subsequent enlarging lesions in RRMS patients and, in patients with SPMS, greater future brain atrophy. Both of these imaging neuropathological changes are associated with disability progression.

Acknowledgements

We would like to thank ICOMETRIX for performing the longitudinal analyses of MRI brain volume and white matter lesion changes. GD is grateful for support as a fellow through the Imperial Wellcome-

Formatted: Font color: Red

13

GlaxoSmithKline Clinical Fellowship Training Scheme. PMM acknowledges generous personal support from Edmond J Safra Foundation and Lily Safra and research funding through the Imperial Biomedical Research Centre, an NIHR Senior Investigator Award and the Medical Research Council.

Funding

We gratefully acknowledge the Wellcome Trust and GlaxoSmithKline for funding for this study provided through the Translational Medicine Training PhD Fellowship Grant.

For Peer Review

Figure legends

Figure 1. Illustrative parametric brain PET [^{11}C]PBR28 distribution volume ratio (DVR) images at baseline (A, D) from two patients with associated T2 FLAIR images at baseline (B, E) and after approximately 1 year (C, F). The top panels (A-C) are from a patient (EDSS 4.0) with high average normal appearing white matter (NAWM) DVR (1.35) (patient MS10 in Table 1). The yellow arrowhead highlights a lesion that enlarged over the observation interval. The bottom panels (D-F) include images from a patient (EDSS 6.0) with low average NAWM DVR (0.88) for whom no enlarging T2 lesions were found between the baseline (E) and follow up (F) MRI scans (patient MS17 in Table 1). The colour bar to the right of the PET images shows the dynamic range of DVR in the images (A, D).

Figure 2. Plots of T2 white matter lesions (WML) [^{11}C]PBR28 distribution volume ratio (DVR) against (A) enlarging T2 WML volume change in relapsing remitting multiple sclerosis patients (RRMS) and (B) either normalised whole brain volume (WBV) atrophy rate or grey matter volume (GMV) atrophy rate in secondary progressive disease (SPMS). The dotted line (A) is the best fit line for the RRMS patients (Spearman's $\rho=0.64$, $p=1\times 10^{-3}$). The unbroken regression line is for GMV atrophy ($\rho=0.96$, $p=5\times 10^{-4}$) and the dashed line is for WBV atrophy ($\rho=0.86$, $p=0.04$) in SPMS patients (B).

Figure 3. Boxplot of the enlarging T2 white matter lesion volume over 1 year of follow up of the multiple sclerosis patients stratified by low (<1.10) and high (>1.10) [^{11}C]PBR28 distribution volume ratio (DVR) in the normal appearing white matter (NAWM) at baseline ($p=0.04$).

Figure 4. At baseline, the white matter [^{11}C]PBR28 distribution volume ratios (DVR) are correlated with MRI whole brain and grey matter volumes. (A) Normal appearing white matter (NAWM) DVR against baseline WBV (Spearman's $\rho= -0.81$, $p=4\times 10^{-5}$). (B) White matter lesions (WML) DVR against baseline WBV ($\rho= -0.74$, $p=4\times 10^{-4}$). (C) NAWM DVR against baseline grey matter (GM) volume ($\rho= -0.56$, $p=0.02$). (D) WML DVR against baseline GM volume ($\rho= -0.42$, $p=0.08$).

Figure 5. Plots of normal appearing white matter (NAWM) [^{11}C]PBR28 distribution volume ratio (DVR) against (A) T2 white matter lesion (WML) DVR (Spearman's $\rho= 0.92$, $p=1\times 10^{-10}$), (B) cortical DVR ($\rho= 0.93$, $p=4\times 10^{-11}$) and (C) thalamic DVR ($\rho= 0.79$, $p=4\times 10^{-6}$).

TABLE 1. Clinical demographics of individual multiple sclerosis ~~patients~~ subjects. Relapses ~~and~~ EDSS change ~~and medication change~~ refer to the time period between baseline and 1 year follow-up visits. ~~Disease duration is the time between the manifestation of patient's first symptoms and the date of MRI examination.~~ The baseline characteristics of these patients have been described in a recent report (Datta *et al.*, 2017). ~~Age and disease duration refer to the time of the baseline visit.~~ Abbreviations: MS = multiple sclerosis; F = female; M = male; RRMS = relapsing remitting multiple sclerosis; SPMS = secondary progressive multiple sclerosis; DMT = disease modifying treatment. ~~Three patients (grey) were assessed only at the baseline, as described earlier (Datta *et al.*, 2017) and were not included in the longitudinal follow up of this cohort that is described in this report.~~

| Patient | Gender | Age (years) | MS subtype | Disease duration (years) | Baseline EDSS | Follow-up EDSS | EDSS change | Relapses | DMT treatment at follow-up (changes from baseline are noted) |
|---------|--------|-------------|------------|--------------------------|---------------|----------------|-------------|----------|--|
| A1 | F | 22 | RRMS | 16 | 3.0 | 3.5 | 0.5 | 3 | Fingolimod |
| A2 | M | 38 | RRMS | 10 | 6.0 | 6.5 | 0.5 | 0 | Alemtuzimab |
| A3 | F | 42 | RRMS | 13 | 1.0 | 1.0 | 0 | 0 | Nataluzimab |
| A4 | F | 50 | RRMS | 9 | 2.5 | 2.0 | -0.5 | 1 | None |
| A5 | M | 59 | SPMS | 23 | 6.0 | 6.0 | 0 | 0 | None |
| A6 | M | 36 | RRMS | 6 | 1.0 | 1.0 | 0 | 1 | Dimethyl fumarate |
| A7 | F | 57 | RRMS | 18 | 1.0 | 1.0 | 0 | 1 | Fingolimod |
| A8 | M | 48 | RRMS | 12 | 7.0 | 7.0 | 0 | 0 | Nataluzimab |
| A9 | M | 53 | RRMS | 14 | 5.0 | | | | Nataluzimab |
| A10 | M | 43 | SPMS | 13 | 5.0 | 5.0 | 0 | 0 | None |
| A11 | F | 29 | RRMS | 1 | 1.0 | 1.0 | 0 | 0 | None (interferon β was discontinued 6 months before follow-up) |
| A12 | F | 51 | RRMS | 8 | 6.5 | 6.5 | 0 | 1 | Nataluzimab |
| A13 | F | 62 | SPMS | 24 | 6.0 | 6.0 | 0 | 0 | None |
| A14 | M | 56 | SPMS | 17 | 7.0 | 7.0 | 0 | 0 | None |
| A15 | F | 52 | RRMS | 6 | 2.0 | 1.5 | -0.5 | 0 | Alemtuzimab |
| A16 | F | 45 | RRMS | 28 | 4.0 | 4.0 | 0 | 0 | Alemtuzimab |
| A17 | F | 66 | SPMS | 17 | 6.5 | 7.5 | 1 | 0 | None |
| A18 | F | 53 | RRMS | 16 | 3.0 | 3.0 | 0 | 0 | None |
| A19 | F | 30 | RRMS | 6 | 4.0 | 5.5 | 1.5 | 1 | None (nataluzimab was discontinued 9 months before follow-up visit) |
| A20 | M | 36 | SPMS | 10 | 7.0 | 7.0 | 0 | 0 | None |
| A21 | M | 47 | SPMS | 11 | 7.0 | 8.0 | 1 | 0 | None |
| A22 | M | 39 | RRMS | 10 | 4.0 | | | | Alemtuzimab |
| A23 | F | 45 | RRMS | 14 | 6.5 | | | | Fingolimod |

16

| | | | | | | | | | |
|-----|---|----|------|----|-----|-----|-----|---|-------------|
| A24 | F | 64 | RRMS | 22 | 2.5 | 3.0 | 0.5 | 0 | Nataluzimab |
|-----|---|----|------|----|-----|-----|-----|---|-------------|

TABLE 2. MRI brain volume characteristics of individual multiple sclerosis ~~patients~~ subjects. Abbreviations: NAWM = normal appearing white matter; MS = multiple sclerosis; WBV = whole brain volume (normalised); GMV = grey matter volume (normalised); T2 WML = T2-weighted white matter lesions. Three patients (grey) were assessed only at the baseline, as described earlier (Datta *et al.*, 2017) and were not included in the longitudinal follow up of this cohort that is described in this report.

| Patient | ¹¹¹ C]PBR28 NAWM DVR | Baseline WBV (cm ³) | Follow-up WBV (cm ³) | WBV change (%) | Baseline GMV (cm ³) | Follow-up GMV (cm ³) | GMV change (%) | Baseline T2 WML volume (mL) | T2 WML volume change (mL) | Enlarging T2 WML volume change (mL) |
|---------|------------------------------------|------------------------------------|-------------------------------------|-------------------|------------------------------------|-------------------------------------|-------------------|-----------------------------------|---------------------------------|---|
| A1 | 0.80 | 1505 | 1493 | -0.85 | 910 | 906 | -1.2 | 4.6 | -0.1 | 0.2 |
| A2 | 0.81 | 1529 | 1537 | 0.56 | 901 | 902 | 0.71 | 1.5 | 0.0 | 0.2 |
| A3 | 0.82 | 1544 | 1531 | -0.3 | 926 | 915 | -0.14 | 5.4 | -0.1 | 0.1 |
| A4 | 0.87 | 1489 | 1485 | 0.16 | 917 | 907 | -0.19 | 2.2 | -0.1 | 0.1 |
| A5 | 0.88 | 1422 | 1407 | -0.16 | 842 | 831 | -0.5 | 6.2 | -0.3 | 0.3 |
| A6 | 0.94 | 1500 | 1505 | 0.5 | 940 | 937 | 0.72 | 6.1 | -0.2 | 0.1 |
| A7 | 0.97 | 1467 | 1465 | -0.52 | 898 | 894 | -0.6 | 2.0 | -0.1 | 0.0 |
| A8 | 1.03 | 1408 | 1410 | 0.57 | 865 | 859 | 0.38 | 14.9 | 0.2 | 0.3 |
| A9 | 1.07 | 1403 | | | 838 | | | 23.4 | | |
| A10 | 1.07 | 1448 | 1433 | 0.11 | 849 | 839 | 0.13 | 9.8 | -0.3 | 0.4 |
| A11 | 1.08 | 1524 | 1513 | -0.13 | 922 | 914 | -0.18 | 8.2 | -0.9 | 0.5 |
| A12 | 1.09 | 1399 | 1412 | -0.78 | 871 | 878 | -1.21 | 4.7 | -0.4 | 0.1 |
| A13 | 1.11 | 1388 | 1390 | -0.21 | 832 | 830 | 0.09 | 8.0 | -0.2 | 0.6 |
| A14 | 1.12 | 1395 | 1392 | 0.21 | 862 | 850 | 0.19 | 5.8 | -0.2 | 0.2 |
| A15 | 1.16 | 1477 | 1478 | 0.21 | 859 | 856 | -0.05 | 13.8 | -1.2 | 0.7 |
| A16 | 1.20 | 1424 | 1417 | -0.12 | 873 | 866 | 0.11 | 29.5 | -1.9 | 2.8 |
| A17 | 1.29 | 1390 | 1372 | 0.02 | 820 | 805 | -0.28 | 36.7 | 2.2 | 2.3 |
| A18 | 1.32 | 1431 | 1426 | -0.5 | 899 | 888 | -0.8 | 15.4 | -0.7 | 0.8 |
| A19 | 1.35 | 1383 | 1366 | -1.39 | 843 | 838 | -0.68 | 26.7 | 0.6 | 1.6 |
| A20 | 1.38 | 1337 | 1370 | 1.45 | 838 | 860 | 2.44 | 20.6 | -0.6 | 0.1 |
| A21 | 1.51 | 1341 | 1343 | 0.5 | 803 | 821 | 1.88 | 8.3 | 0.2 | 0.4 |
| A22 | 1.67 | 1361 | | | 842 | | | 38.1 | | |
| A23 | 1.68 | 1440 | | | 903 | | | 2.3 | | |
| A24 | 1.85 | 1251 | 1246 | -0.61 | 790 | 789 | -0.52 | 36.6 | 0.5 | 3.4 |

References

- Absinta M, Vuolo L, Rao A, Nair G, Sati P, Cortese IC, *et al.* Gadolinium-based MRI characterization of leptomeningeal inflammation in multiple sclerosis. *Neurology* 2015; 85(1): 18-28.
- Agosta F, Rovaris M, Pagani E, Sormani MP, Comi G, Filippi M. Magnetization transfer MRI metrics predict the accumulation of disability 8 years later in patients with multiple sclerosis. *Brain* 2006; 129(Pt 10): 2620-7.
- Allen IV, McQuaid S, Mirakhur M, Nevin G. Pathological abnormalities in the normal-appearing white matter in multiple sclerosis. *Neurol Sci* 2001; 22(2): 141-4.
- Barkhof F, Calabresi PA, Miller DH, Reingold SC. Imaging outcomes for neuroprotection and repair in multiple sclerosis trials. *Nat Rev Neurol* 2009; 5(5): 256-66.
- Battaglini M, Jenkinson M, De Stefano N. Evaluating and reducing the impact of white matter lesions on brain volume measurements. *Hum Brain Mapp* 2012; 33(9): 2062-71.
- Bo L, Geurts JJ, van der Valk P, Polman C, Barkhof F. Lack of correlation between cortical demyelination and white matter pathologic changes in multiple sclerosis. *Arch Neurol* 2007; 64(1): 76-80.
- Briard E, Zoghbi SS, Imaizumi M, Gourley JP, Shetty HU, Hong J, *et al.* Synthesis and evaluation in monkey of two sensitive ¹¹C-labeled aryloxyanilide ligands for imaging brain peripheral benzodiazepine receptors in vivo. *J Med Chem* 2008; 51(1): 17-30.
- Calabrese M, Magliozzi R, Ciccarelli O, Geurts JJ, Reynolds R, Martin R. Exploring the origins of grey matter damage in multiple sclerosis. *Nat Rev Neurosci* 2015; 16(3): 147-58.
- Colasanti A, Guo Q, Muhlert N, Giannetti P, Onega M, Newbould RD, *et al.* In Vivo Assessment of Brain White Matter Inflammation in Multiple Sclerosis with (18)F-PBR111 PET. *J Nucl Med* 2014; 55(7): 1112-8.
- Cosenza-Nashat M, Zhao ML, Suh HS, Morgan J, Natividad R, Morgello S, *et al.* Expression of the translocator protein of 18 kDa by microglia, macrophages and astrocytes based on immunohistochemical localization in abnormal human brain. *Neuropathol Appl Neurobiol* 2009; 35(3): 306-28.
- Datta G, Colasanti A, Kalk N, Owen DR, Scott G, Rabiner EI, *et al.* [¹¹C]PBR28 or [¹⁸F]PBR111 detect white matter inflammatory heterogeneity in multiple sclerosis. *J Nucl Med* 2017.
- Datta G, Violante IR, Scott G, Zimmerman K, Santos-Ribeiro A, Rabiner EA, *et al.* Translocator positron-emission tomography and magnetic resonance spectroscopic imaging of brain glial cell activation in multiple sclerosis. *Mult Scler* 2016.
- Duffy SS, Lees JG, Moalem-Taylor G. The contribution of immune and glial cell types in experimental autoimmune encephalomyelitis and multiple sclerosis. *Mult Scler Int* 2014; 2014: 285245.
- Filippi M, Paty DW, Kappos L, Barkhof F, Compston DA, Thompson AJ, *et al.* Correlations between changes in disability and T2-weighted brain MRI activity in multiple sclerosis: a follow-up study. *Neurology* 1995; 45(2): 255-60.

- Filippi M, Rocca MA, Barkhof F, Bruck W, Chen JT, Comi G, *et al.* Association between pathological and MRI findings in multiple sclerosis. *Lancet Neurol* 2012; 11(4): 349-60.
- Geurts JJ, Bo L, Pouwels PJ, Castelijns JA, Polman CH, Barkhof F. Cortical lesions in multiple sclerosis: combined postmortem MR imaging and histopathology. *AJNR Am J Neuroradiol* 2005; 26(3): 572-7.
- Giannetti P, Politis M, Su P, Turkheimer FE, Malik O, Keihaninejad S, *et al.* Increased PK11195-PET binding in normal-appearing white matter in clinically isolated syndrome. *Brain* 2015; 138(Pt 1): 110-9.
- Goldman MD, Motl RW, Rudick RA. Possible clinical outcome measures for clinical trials in patients with multiple sclerosis. *Ther Adv Neurol Disord* 2010; 3(4): 229-39.
- Gourraud PA, Sdika M, Khankhanian P, Henry RG, Beheshtian A, Matthews PM, *et al.* A genome-wide association study of brain lesion distribution in multiple sclerosis. *Brain* 2013; 136(Pt 4): 1012-24.
- Herranz E, Gianni C, Louapre C, Treaba CA, Govindarajan ST, Ouellette R, *et al.* Neuroinflammatory component of gray matter pathology in multiple sclerosis. *Ann Neurol* 2016; 80(5): 776-90.
- Jack CR, Jr., Bernstein MA, Fox NC, Thompson P, Alexander G, Harvey D, *et al.* The Alzheimer's Disease Neuroimaging Initiative (ADNI): MRI methods. *J Magn Reson Imaging* 2008; 27(4): 685-91.
- Jain S, Sima DM, Ribbens A, Cambron M, Maertens A, Van Hecke W, *et al.* Automatic segmentation and volumetry of multiple sclerosis brain lesions from MR images. *Neuroimage Clin* 2015; 8: 367-75.
- Klaver R, De Vries HE, Schenk GJ, Geurts JJ. Grey matter damage in multiple sclerosis: a pathology perspective. *Prion* 2013; 7(1): 66-75.
- Lee MA, Smith S, Palace J, Matthews PM. Defining multiple sclerosis disease activity using MRI T2-weighted difference imaging. *Brain* 1998; 121 (Pt 11): 2095-102.
- Logan J, Fowler JS, Volkow ND, Wang GJ, Ding YS, Alexoff DL. Distribution volume ratios without blood sampling from graphical analysis of PET data. *J Cereb Blood Flow Metab* 1996; 16(5): 834-40.
- Lucchinetti CF, Bruck W, Lassmann H. Evidence for pathogenic heterogeneity in multiple sclerosis. *Ann Neurol* 2004; 56(2): 308.
- Lucchinetti CF, Popescu BF, Bunyan RF, Moll NM, Roemer SF, Lassmann H, *et al.* Inflammatory cortical demyelination in early multiple sclerosis. *N Engl J Med* 2011; 365(23): 2188-97.
- Matthews PM, Datta G. Positron-emission tomography molecular imaging of glia and myelin in drug discovery for multiple sclerosis. *Expert Opin Drug Discov* 2015; 10(5): 557-70.
- Moll NM, Rietsch AM, Thomas S, Ransohoff AJ, Lee JC, Fox R, *et al.* Multiple sclerosis normal-appearing white matter: pathology-imaging correlations. *Ann Neurol* 2011; 70(5): 764-73.
- Mowry EM, Waubant E, McCulloch CE, Okuda DT, Evangelista AA, Lincoln RR, *et al.* Vitamin D status predicts new brain magnetic resonance imaging activity in multiple sclerosis. *Ann Neurol* 2012; 72(2): 234-40.
- Owen DR, Yeo AJ, Gunn RN, Song K, Wadsworth G, Lewis A, *et al.* An 18-kDa translocator protein (TSPO) polymorphism explains differences in binding affinity of the PET radioligand PBR28. *J Cereb Blood Flow Metab* 2012; 32(1): 1-5.

- Politis M, Giannetti P, Su P, Turkheimer F, Keihaninejad S, Wu K, *et al.* Increased PK11195 PET binding in the cortex of patients with MS correlates with disability. *Neurology* 2012; 79(6): 523-30.
- Polman CH, Reingold SC, Banwell B, Clanet M, Cohen JA, Filippi M, *et al.* Diagnostic criteria for multiple sclerosis: 2010 revisions to the McDonald criteria. *Ann Neurol* 2011; 69(2): 292-302.
- Popescu BF, Lucchinetti CF. Meningeal and cortical grey matter pathology in multiple sclerosis. *BMC Neurol* 2012; 12: 11.
- Popescu V, Agosta F, Hulst HE, Sluimer IC, Knol DL, Sormani MP, *et al.* Brain atrophy and lesion load predict long term disability in multiple sclerosis. *J Neurol Neurosurg Psychiatry* 2013; 84(10): 1082-91.
- Prineas JW, Kwon EE, Cho ES, Sharer LR, Barnett MH, Oleszak EL, *et al.* Immunopathology of secondary-progressive multiple sclerosis. *Ann Neurol* 2001; 50(5): 646-57.
- Rissanen E, Tuisku J, Rokka J, Paavilainen T, Parkkola R, Rinne JO, *et al.* In Vivo Detection of Diffuse Inflammation in Secondary Progressive Multiple Sclerosis Using PET Imaging and the Radioligand (1)(1)C-PK11195. *J Nucl Med* 2014; 55(6): 939-44.
- Schmierer K, Scaravilli F, Altmann DR, Barker GJ, Miller DH. Magnetization transfer ratio and myelin in postmortem multiple sclerosis brain. *Ann Neurol* 2004; 56(3): 407-15.
- Seewann A, Vrenken H, van der Valk P, Blezer EL, Knol DL, Castelijns JA, *et al.* Diffusely abnormal white matter in chronic multiple sclerosis: imaging and histopathologic analysis. *Arch Neurol* 2009; 66(5): 601-9.
- Singh S, Metz I, Amor S, van der Valk P, Stadelmann C, Bruck W. Microglial nodules in early multiple sclerosis white matter are associated with degenerating axons. *Acta Neuropathol* 2013; 125(4): 595-608.
- Smeets D, Ribbens A, Sima DM, Cambron M, Horakova D, Jain S, *et al.* Reliable measurements of brain atrophy in individual patients with multiple sclerosis. *Brain Behav* 2016; 6(9): e00518.
- Smith SM, Zhang Y, Jenkinson M, Chen J, Matthews PM, Federico A, *et al.* Accurate, robust, and automated longitudinal and cross-sectional brain change analysis. *Neuroimage* 2002; 17(1): 479-89.
- Sormani MP, Arnold DL, De Stefano N. Treatment effect on brain atrophy correlates with treatment effect on disability in multiple sclerosis. *Ann Neurol* 2014; 75(1): 43-9.
- Sormani MP, Bonzano L, Roccatagliata L, De Stefano N. Magnetic resonance imaging as surrogate for clinical endpoints in multiple sclerosis: data on novel oral drugs. *Mult Scler* 2011; 17(5): 630-3.
- Tziortzi AC, Searle GE, Tzimopoulou S, Salinas C, Beaver JD, Jenkinson M, *et al.* Imaging dopamine receptors in humans with [11C]-(+)-PHNO: dissection of D3 signal and anatomy. *Neuroimage* 2011; 54(1): 264-77.
- van Horssen J, Singh S, van der Pol S, Kipp M, Lim JL, Peferoen L, *et al.* Clusters of activated microglia in normal-appearing white matter show signs of innate immune activation. *J Neuroinflammation* 2012; 9: 156.

20

Versijpt J, Debruyne JC, Van Laere KJ, De Vos F, Keppens J, Strijckmans K, *et al.* Microglial imaging with positron emission tomography and atrophy measurements with magnetic resonance imaging in multiple sclerosis: a correlative study. *Mult Scler* 2005; 11(2): 127-34.

Vrenken H, Geurts JJ, Knol DL, Polman CH, Castelijns JA, Pouwels PJ, *et al.* Normal-appearing white matter changes vary with distance to lesions in multiple sclerosis. *AJNR Am J Neuroradiol* 2006; 27(9): 2005-11.

Zivadinov R, Weinstock-Guttman B, Hashmi K, Abdelrahman N, Stosic M, Dwyer M, *et al.* Smoking is associated with increased lesion volumes and brain atrophy in multiple sclerosis. *Neurology* 2009; 73(7): 504-10.

For Peer Review

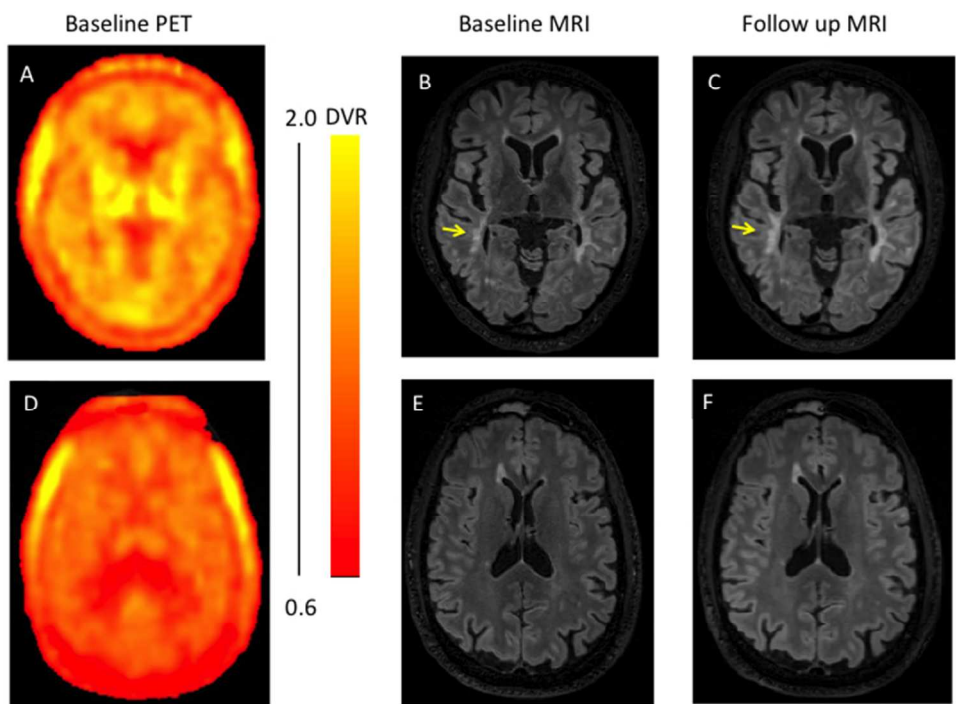


Figure 1

254x190mm (72 x 72 DPI)

review

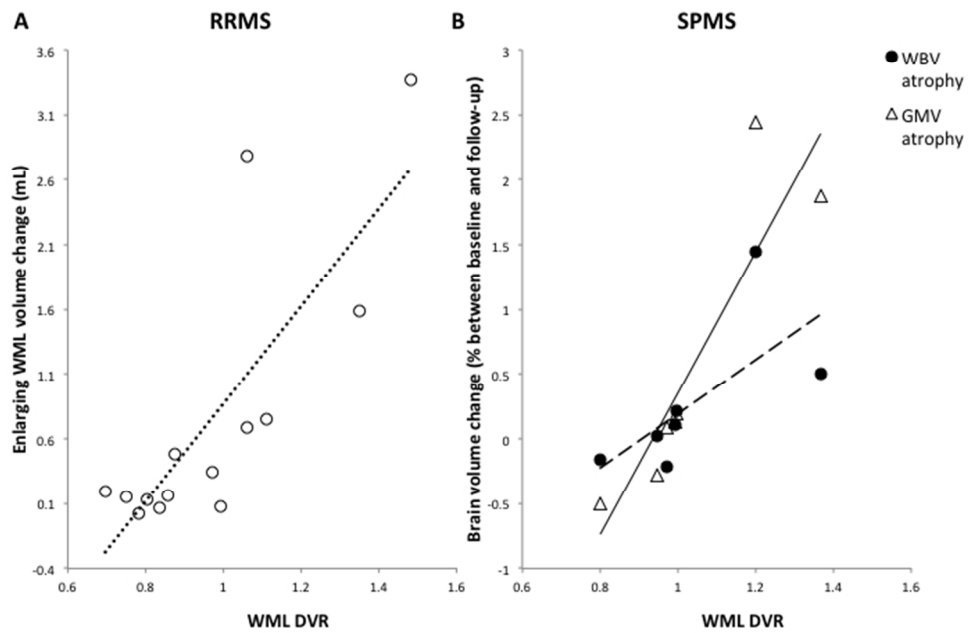


Figure 2

254x190mm (72 x 72 DPI)

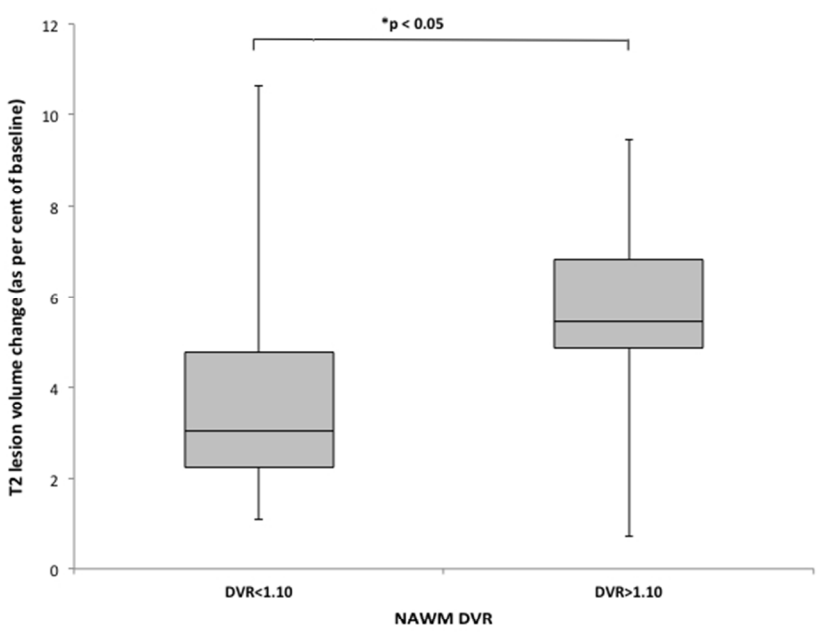


Figure 3

254x190mm (72 x 72 DPI)

Review

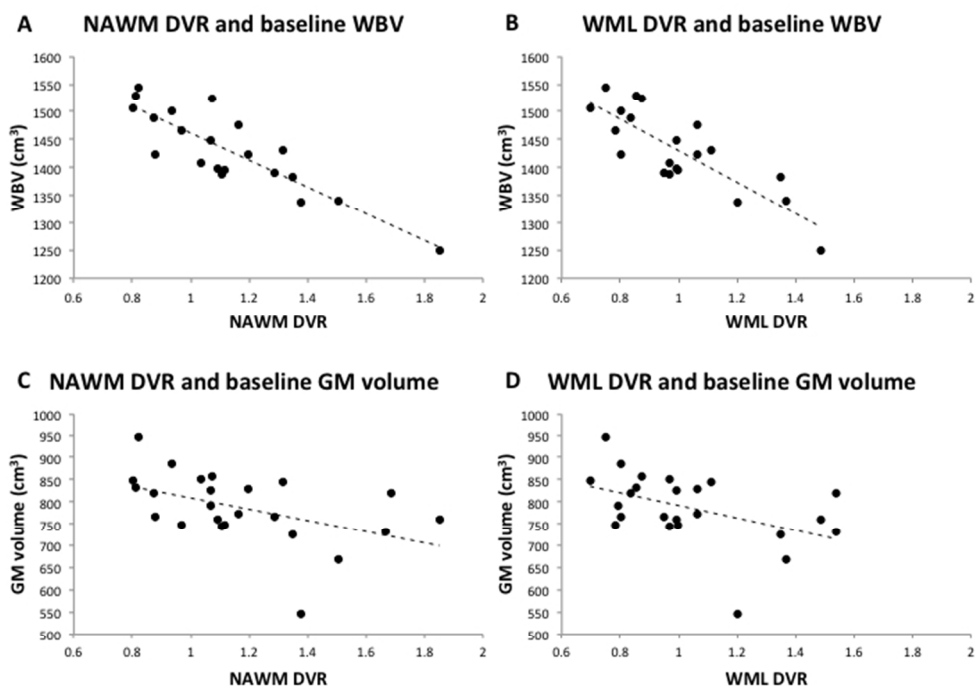


Figure 4

254x190mm (72 x 72 DPI)

Review

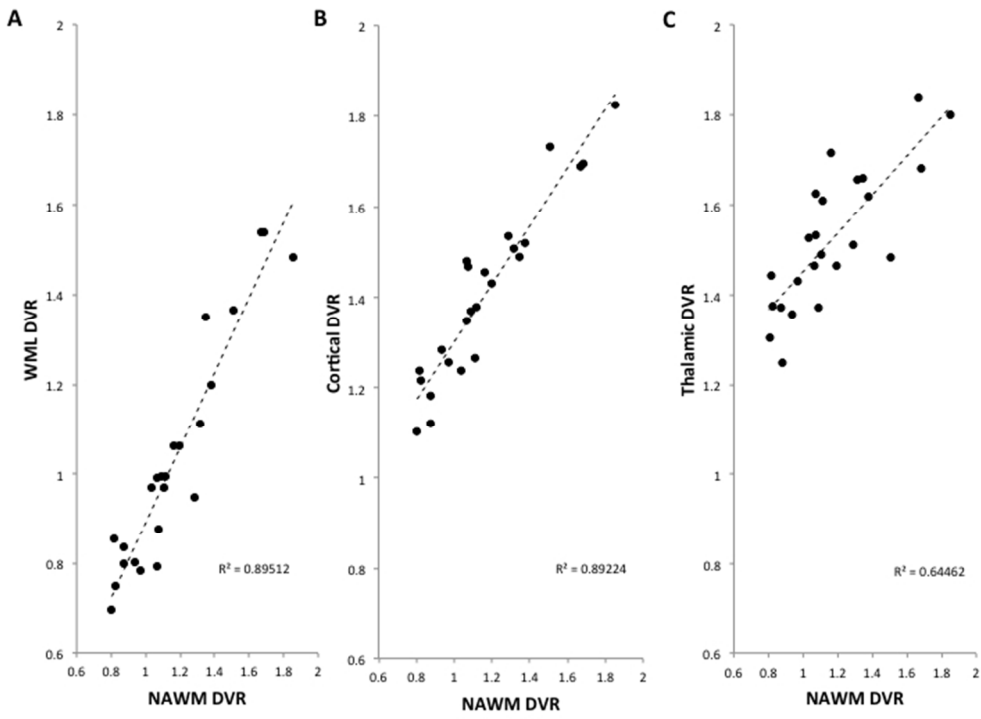
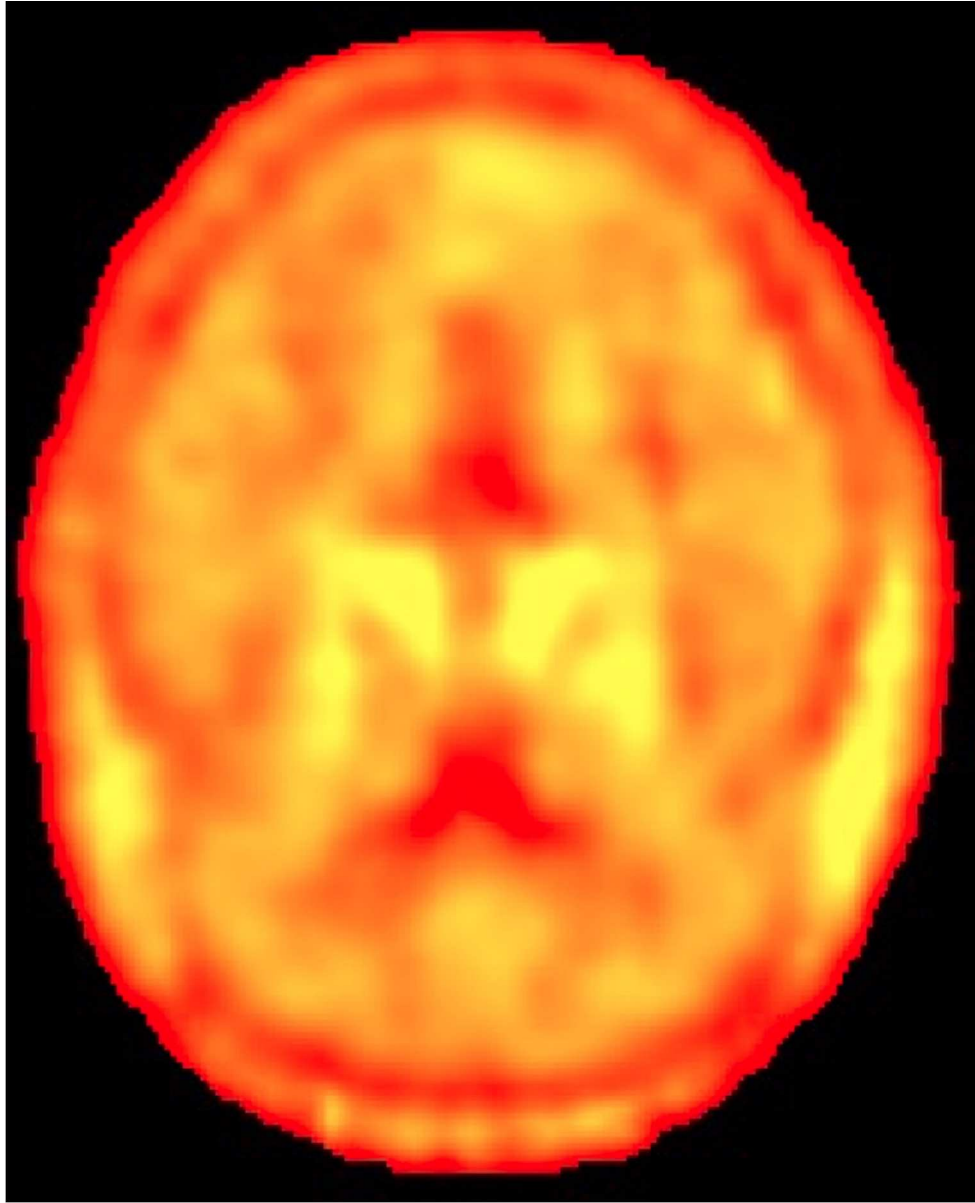


Figure 5

254x190mm (72 x 72 DPI)

Review



238x294mm (144 x 144 DPI)